

Synthesis and Thermal and Wetting Properties of Tin/Silver Alloy Nanoparticles for Low Melting Point Lead-Free Solders

Hongjin Jiang,[†] Kyoung-sik Moon,[†] Fay Hua,[‡] and C. P. Wong^{*,†}

School of Materials Science and Engineering and School of Chemistry and Biochemistry, Georgia Institute of Technology, Atlanta, Georgia 30332, and Materials Technology Operation, Intel Corporation, 3065 Bowers Avenue, Santa Clara, California 95054

Received April 11, 2007. Revised Manuscript Received June 20, 2007

Tin/silver alloy nanoparticles with various sizes were synthesized via a low-temperature chemical reduction method, and their thermal properties were studied by differential scanning calorimetry. The particle size dependency of the melting temperature and the latent heat of fusion was observed. The melting point was achieved as low as 194 °C when the average diameter of the alloy nanoparticles was around 10 nm. The wetting test for as-prepared 64 nm (average diameter) SnAg alloy nanoparticle pastes on a Cu surface showed the typical Cu₆Sn₅ intermetallic compound (IMC) formation. These low melting point SnAg alloy nanoparticles could be used for low-temperature lead-free interconnect applications.

Introduction

Tin/lead (Sn/Pb) eutectic solders have long been used as an electrical interconnect material in the electronic packaging field. Lead, one of the components in the solder, has been recognized as a health threat to human beings and the natural environment. Due to these concerns, the investigation of an alternative to make lead-free solder is imperative. Tin/silver (96.5Sn–3.5Ag) is one of the promising alternatives for Sn/Pb solders.¹ However, the melting point (T_m) of 96.5Sn–3.5Ag alloy is more than 30 °C higher than that of eutectic Sn/Pb solders. The higher T_m requires the higher reflow temperature in the electronics manufacturing process, which has adverse effects not only on energy consumption but also on the package reliability, such as substrate warpage, thermal stress, and popcorn cracking in molding compounds. Therefore, industry's attentions have been paid to lowering the processing temperature of the lead-free metals.

The melting point can be dramatically decreased when the size of the substances is reduced to nanometer size.² To date, the size-dependent melting behavior has been found both theoretically and experimentally.^{3–9} The high ratio of the surface area to volume of nanoparticles has been known as one of the driving forces for the size-dependent melting point depression.

Hsiao and Duh have reported Sn–3.5Ag– x Cu ($x = 0.2, 0.5, 1.0$) nanoparticles synthesis for the lead-free solder application,¹⁰ where the differential scanning calorimetry (DSC) profile showed the melting (endothermic) peak of their SnAgCu alloy nanoparticles at ~216 °C, which is the melting point of the micrometer-sized SnAgCu alloy powders. No obvious melting point depression from their particles might be due to the surface oxidation or heavy agglomeration of the nanoparticles.

Transmission electron microscopy (TEM), a nanocalorimeter, and DSC have been used to study the melting behavior of non-noble metal nanoparticles or clusters, such as tin nanoparticles. In the TEM characterizations, at the melting point the diffraction pattern of the crystal structure exhibited an order–disorder transition.¹¹ However, it could not measure the latent heat of fusion (ΔH_m). Therefore, the nanocalorimeter was used to investigate the melting process of Sn nanoclusters.³ It was found that the melting point depended nonlinearly on the inverse of the cluster radius. And a particle-size-dependent reduction of ΔH_m for Sn nanoparticles was first found by the nanocalorimetric technique. However, for both the TEM and nanocalorimetric measurements, a single Sn nanoparticle or a cluster was synthesized by the deposition method inside the equipment directly in order to prevent oxidation of the particles. Although these synthesis methods were sufficiently sophisticated for the pure observation, the real world synthesis and characterization possess more experimental parameters to consider, such as oxidation during moving of samples. Our group has reported the synthesis of Sn nanoparticles which were protected from oxidation by particle surface capping, and their melting point depression behavior was first studied by conventional DSC.¹²

In this study, a low-temperature chemical reduction method was used to synthesize different-size SnAg alloy nanoparticles for lead-free solder applications. The average diameter of the particles can be achieved down to 10 nm. Surfactants/

* Corresponding author. E-mail: cp.wong@mse.gatech.edu.

[†] Georgia Institute of Technology.

[‡] Intel Corp.

- (1) Artaki, I.; Jackson, A. M.; Vianco, P. T. *J. Electron. Mater.* **1994**, *23*, 757.
- (2) Pawlow, P. Z. *Phys. Chem.* **1909**, *65*, 1.
- (3) Lai, S. L.; Guo, J. Y.; Petrova, V.; Ramanath, G.; Allen, L. H. *Phys. Rev. Lett.* **1996**, *77*, 99.
- (4) Bachelis, T.; Guntherodt, H. J.; Schafer, R. *Phys. Rev. Lett.* **2000**, *85*, 1250.
- (5) Kofman, R.; Cheyssac, P.; Celestini, F. *Phys. Rev. Lett.* **2001**, *86*, 1388.
- (6) Schmidt, M.; Kusche, R.; Issendorff, B.; Haberland, H. *Nature* **1998**, *393*, 238.
- (7) Zhao, S. J.; Wang, D. Y.; Cheng, H. Q.; Ye, H. Q. *J. Phys. Chem. B* **2001**, *105*, 12857.
- (8) Baletto, F.; Rapallo, A.; Rossi, G.; Ferrando, R. *Phys. Rev. B* **2004**, *69*, 235421.
- (9) Shi, F. G. *J. Mater. Res.* **1994**, *9*, 1307.

(10) Hsiao, L. Y.; Duh, J. G. *J. Electrochem. Soc.* **2005**, *152*, J105.

(11) Buffat, P.; Borel, J. P. *Phys. Rev. A* **1976**, *13*, 2287.

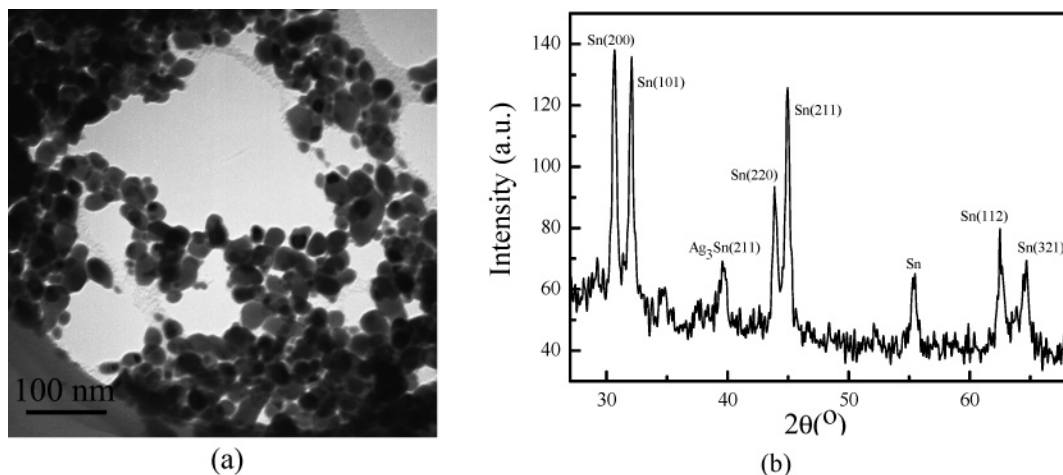


Figure 1. TEM image (a) and XRD patterns (b) of the SnAg alloy nanoparticles which were synthesized by using 7.4×10^{-4} mol of tin(II) 2-ethylhexanoate and 3.0×10^{-5} mol of silver nitrate as precursors in the presence of 5.6×10^{-4} mol of surfactants.

stabilizing agents were employed to prevent oxidation of the synthesized SnAg alloy nanoparticles. The microstructures of the synthesized SnAg nanoparticles were characterized by X-ray diffraction (XRD) and high-resolution transmission electron microscopy (HRTEM), and the thermal behaviors of the nanoparticles were studied by conventional DSC. In addition, the wetting test result for nanosolder pastes filled with the as-synthesized 64 nm (average diameter) SnAg alloy nanoparticles was discussed.

Experimental Section

1. Materials. Tin(II) 2-ethylhexanoate, silver nitrate, sodium borohydride, 1,10-phenanthroline,¹³ and anhydrous methanol were used as precursors, reducing agents, surfactants, and solvents, respectively. These chemicals were all purchased from Aldrich and used without further purification.

2. Synthesis. In a typical experiment, 7.4×10^{-4} mol of tin(II) 2-ethylhexanoate, 3.0×10^{-5} mol of silver nitrate (weight ratio of Sn/Ag \approx 96.5/3.5) and 5.6×10^{-4} mol of 1,10-phenanthroline¹³ were mixed into a 60 mL anhydrous methanol solution. The solution was stirred and nitrogen-purged for 2 h. Thereafter, 5.0×10^{-3} mol of sodium borohydride was added to the solution and the reaction continued for 1 h at 0 °C. The as-prepared nanoparticles in solution were centrifuged at 4000 rpm for 15 min, then washed with methanol for three times, and dried in a vacuum oven for 24 h at room temperature. After drying, the powders were stored in a nitrogen box.

3. Characterization. Transmission electron microscopy (JEOL 100C TEM) was used to observe the morphologies of the synthesized nanoparticles. TEM specimens were prepared by dispersing a few drops of the SnAg alloy nanoparticle solution onto a carbon film supported by copper grids. X-ray diffraction (PW 1800) and high-resolution transmission electron microscopy (Hitachi 2000K TEM) were used to study the crystal structure of SnAg alloy nanoparticles. A thermogravimetric analyzer (TGA, 2050 from Thermal Advantages Inc.) was used to investigate the thermal degradation of the surfactants anchoring on the SnAg nanoparticle surface. The melting point of the SnAg alloy nanoparticles was determined by a differential scanning calorimeter (TA Instruments, model 2970). A sample of about 5.0 mg was hermetically sealed into an aluminum pan and placed in the DSC cell under nitrogen purge. Dynamic scans were made on the samples at a heating rate

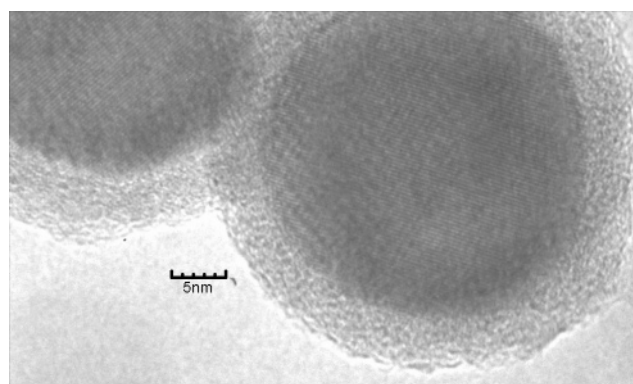


Figure 2. HRTEM image of SnAg alloy nanoparticles which were synthesized by using 7.4×10^{-4} mol of tin(II) 2-ethylhexanoate and 3.0×10^{-5} mol of silver nitrate as precursors in the presence of 5.6×10^{-4} mol of surfactants.

of 5 °C/min, from room temperature to 250 °C. Thereafter, the sample was cooled to room temperature at a cooling rate of 5 °C/min. The cross-section of solders on a copper foil surface after reflow was studied by scanning electron microscopy (SEM), and energy dispersion spectrometry (EDS) was used to study the composition of the IMC. The SEM is a Hitachi S-800 equipped with a thermally assisted field emission gun operating at 10 KeV.

Results and Discussion

1. Synthesis and Thermal Properties of SnAg Alloy Nanoparticles. Figure 1a shows the TEM image of the SnAg alloy nanoparticles synthesized by using 7.4×10^{-4} mol of tin(II) 2-ethylhexanoate and 3.0×10^{-5} mol of silver nitrate as precursors in the presence of 5.6×10^{-4} mol of surfactants at 0 °C. The average diameter of the particles was \sim 24.0 nm. The XRD patterns of the as-synthesized SnAg alloy nanoparticles are shown in Figure 1b. In addition to the peaks indexed to a tetragonal cell of Sn with $a = 0.582$ and $c = 0.317$ nm, the Ag₃Sn phase (\sim 39.6°) was found in the XRD patterns, indicating the successful alloying of Sn and Ag after the reduction process.^{10,14} No prominent oxide peak was observed from the XRD patterns. This indicates that the surfactants could help to protect the synthesized SnAg alloy nanoparticles from oxidation.^{12,15}

Figure 2 shows the HRTEM image of the as-synthesized SnAg alloy nanoparticles, where the particles showed core–

(12) Jiang, H. J.; Moon, K.; Dong, H.; Hua, F.; Wong, C. P. *Chem. Phys. Lett.* **2006**, 429, 492.

(13) Jiang, H. J.; Moon, K. S.; Wong, C. P. U.S. patent pending.

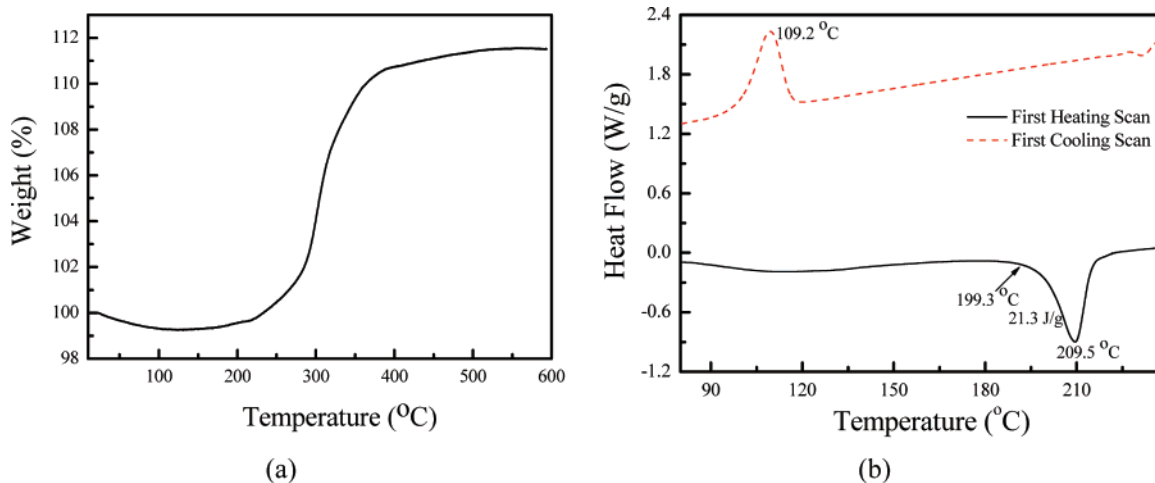


Figure 3. TGA (a) and DSC (b) curves of the SnAg alloy nanoparticles which were synthesized by using 7.4×10^{-4} mol of tin(II) 2-ethylhexanoate and 3.0×10^{-5} mol of silver nitrate as precursors in the presence of 5.6×10^{-4} mol of surfactants.

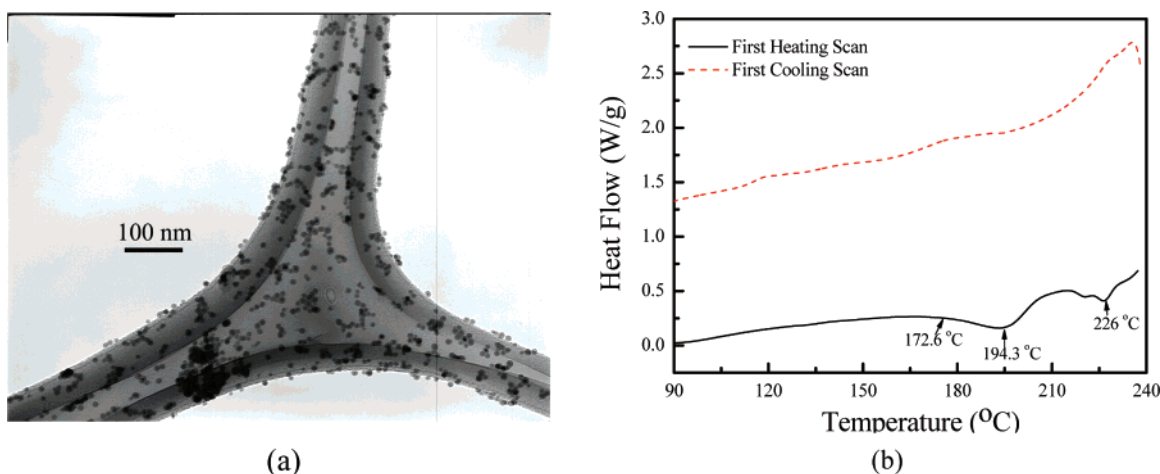


Figure 4. TEM image (a) and DSC curves (b) of the SnAg alloy nanoparticles which were synthesized by using 7.4×10^{-4} mol of tin(II) 2-ethylhexanoate and 3.0×10^{-5} mol of silver nitrate as precursors in the presence of 1.1×10^{-3} mol of surfactants.

shell structures. The dark core and the brighter shell correspond to the crystalline metal and the amorphous organic surfactants, respectively. The surfactant shells on the particle surface protected the SnAg alloy nanoparticles from oxidation.

Figure 3a shows the TGA curve of the dried SnAg alloy nanoparticles in nitrogen atmosphere. The weight loss below 180 °C might be due to the evaporation of a small amount of absorbed moisture and surfactants. Above 180 °C, the weight gain was observed, which was attributed to thermal oxidation of the SnAg alloy nanoparticles. Figure 3b displays the thermal profile of the dried SnAg alloy nanoparticles. The melting point of the SnAg nanoparticles was found at ~ 209.5 °C, about 13 °C lower than that of the micrometer-sized 96.5Sn–3.5Ag particles (222.6 °C). This was an obvious size-dependent melting point depression. ΔH_m of the SnAg alloy nanoparticles (24.2 J/g) was smaller than that of micrometer-sized 96.5Sn–3.5Ag powders (68.6 J/g). It has already been observed by experiments that the normalized heat of fusion of Sn nanoparticles decreases markedly from the bulk value by as much as 70% when the particle

size is reduced. This can be interpreted as a solid core melting following the gradual surface melting for small particles.³ The recrystallization peak of the as-synthesized SnAg alloy nanoparticles was found at 109.2 °C, which was 91.2 °C lower than that of the micrometer-sized 96.5Sn–3.5Ag particles (200.4 °C). Such a supercooling effect in the recrystallization of the melted Sn nanoparticles has already been observed,¹⁶ which can be explained by the critical-sized stable grain that has to form for solidification to take place.¹⁷ Solidification of the melted nanoparticles can only occur once the temperature is low enough so that the critical-size solidification grain can be accommodated in the small volume.

The TEM image and the corresponding DSC curves of SnAg alloy nanoparticles which were synthesized by using 7.4×10^{-4} mol of tin(II) 2-ethylhexanoate and 3.0×10^{-5} mol of silver nitrate as precursors in the presence of 1.1×10^{-3} mol of surfactants at ~ -20 °C are shown in Figure 4a,b. The average diameter of the as-synthesized nanoparticles was ~ 10 nm (Figure 4a). From the DSC studies, the first peak melting temperature was 194.3 °C, which was

(14) Lai, H. L.; Duh, J. G. *J. Electron. Mater.* **2003**, *32*, 215.

(15) Balan, L.; Schneider, R.; Billaud, D.; Ghanbaja, J. *Nanotechnology* **2005**, *16*, 1153.

(16) Banhart, F.; Hernandez, E.; Terrones, M. *Phys. Rev. Lett.* **2003**, *90*, 185502–1.

(17) Christenson, H. K. *J. Phys.: Condens. Matter.* **2001**, *13*, R95.

Table 1. Melting Points and Heat of Fusion of the As-Synthesized Different-Sized SnAg Alloy Nanoparticles^a

no.	surfactants (mol)	reacn temp (°C)	av diam (nm)	melting point (°C)	ΔH_m (J/g)
1	5.6×10^{-4}	25	64	220.0	44.7
2	5.6×10^{-4}	0	24	209.5	24.2
3	8.0×10^{-4}	~ -10	17	206.0	15.1
4	1.1×10^{-3}	~ -20	10	194.3	9.95

^a The melting point and latent heat of fusion for micrometer-sized 96.5Sn–3.5Ag are 222.6 °C and 68.5 J/g, respectively.

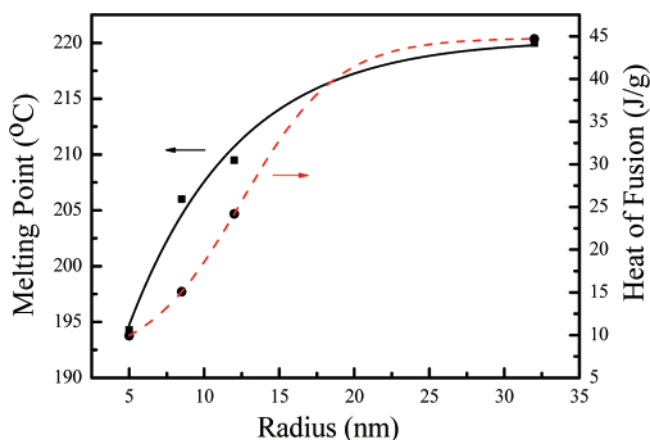


Figure 5. Relationship between the radius of the as-synthesized SnAg alloy nanoparticles and their corresponding melting points and heat of fusion, respectively.

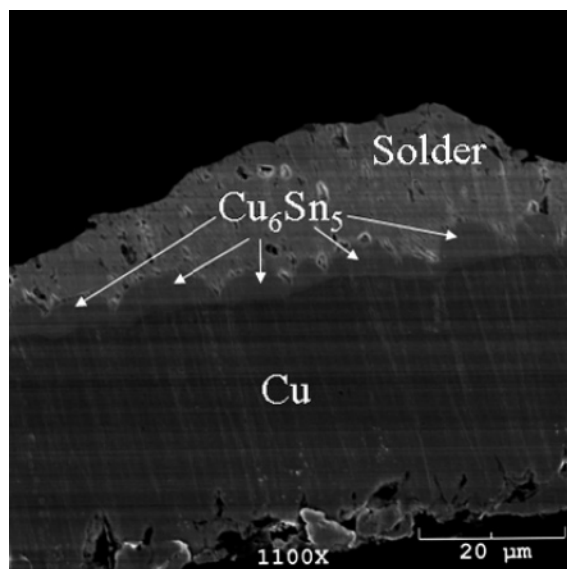


Figure 6. SEM image of the cross-section of the wetted SnAg alloy nanoparticles (sample 1 in Table 1) on the cleaned copper foil.

about 28.3 °C lower than that of micrometer-sized 96.5Sn–3.5Ag particles. The onset peak temperature was 172.6 °C, which was 46.9 °C lower than that of micromete-sized particles (219.5 °C). The melting transition of this sample took place over a temperature range of about 21.7 °C, much wider than the micrometer-sized particles (3.1 °C). This phenomenon can be attributed to a broadening of the phase transition due to the finite size effect.¹⁸ A small peak at 226.0 °C was also observed in the first heating scan, which might come from the melting of a very small amount of larger sized particles existing in this sample.

Table 1 shows the melting point and latent heat of fusion of different-sized SnAg alloy nanoparticles. We plotted the melting point and ΔH_m vs the corresponding particle radius in Figure 5. Both the particle size-dependent melting point depression and latent heat of fusion have been observed. This is due to the surface premelting of nanoparticles. It has already been found that surface melting of small particles occurs in a continuous manner over a broad temperature range, whereas the homogeneous melting of the solid core occurs abruptly at T_m .^{19,20} For smaller size metal nanoparticles, the surface melting is strongly enhanced by curvature effects. Therefore with the decreasing of particle size, both the melting point and latent heat of fusion will decrease too. Among all the synthesized particles in Table 1, the 10 nm (average diameter) SnAg alloy nanoparticles have a melting point at ~ 194.3 °C, which will be a good candidate for the low melting temperature lead-free solders and can solve the issues from the high-temperature reflow for the micrometer-sized lead-free particles.

2. Preliminary Studies on the Wetting Properties of the Synthesized SnAg Alloy Nanoparticles. The SnAg alloy nanoparticles (sample 1 in Table 1) were mixed with an acidic type flux to form the nanosolder pastes at room temperature. A copper foil was cleaned by hydrochloric acid to get rid of the oxide layer and then rinsed with DI water for 4 times. Thereafter, the nanosolder pastes placed on top of the copper foil were put into a 240 °C oven in an air atmosphere for 5 min. The cross-section of the sample after reflow was shown in Figure 6. It was observed that the SnAg alloy nanoparticles completely melted and wetted on the cleaned copper foil surface. The energy dispersive spectroscopy (EDS) results revealed the formation of the IMC (Cu_6Sn_5), which showed scallop-like morphologies in Figure 6. The thickness of the IMC was approximately 4.0 μm . Further studies on the wetting properties of different-sized SnAg alloy nanoparticles at different reflow temperatures are still ongoing.

Conclusion

SnAg alloy nanoparticles with various sizes were successfully synthesized for lead-free solder applications by the chemical reduction method. Surfactants were used to prevent the synthesized SnAg nanoparticles from oxidation. Both the size-dependent melting point and latent heat of fusion were observed from the DSC profiles. The nanosolder paste made of the as-synthesized (~ 64 nm) SnAg alloy nanoparticles was spread and wet on the Cu surface, and the IMC (Cu_6Sn_5) was formed after the reflow process. This study demonstrated the viability of the SnAg alloy nanoparticles as a candidate for the low-temperature lead-free interconnect applications.

Acknowledgment. The authors would like to thank Intel for the financial support.

CM0709976

(18) Imry, Y.; Bergman, D. *Phys. Rev. A* **1971**, *3*, 1416.

(19) Garrigos, R.; Cheyssac, P.; Kofman, R. Z. *Phys. D* **1989**, *12*, 497.

(20) Hu, W. Y.; Xiao, S. F.; Yang, J. Y.; Zhang, Z. *Eur. Phys. J. B* **2005**, *45*, 547.